ISSN 1028-334X, Doklady Earth Sciences, 2025, Vol. 523:25. © Pleiades Publishing, Ltd., 2025.

LITHOLOGY

Lithological Composition of Bottom Sediments in the Area of Fluid Discharge in the Kara Sea

E. A. Moroz[a,*], E. A. Eremenko[a,b], A. V. Ermakov[a], A. P. Denisova[a], A. V. Drazdova[a], R. A. Ananiev[c], V. V. Arkhipov[d], and S. V. Maznev[e]

[a]*Geological Institute, Russian Academy of Sciences, Moscow, 119017 Russia*
[b]*Faculty of Geography, Moscow State University, Moscow, 119991 Russia*
[c]*Shirshov Institute of Oceanology, Russian Academy of Sciences, Moscow, 117997 Russia*
[d]*Zubov State Oceanographic Institute, Moscow, 119034 Russia*
[e]*Al-Farabi Kazakh National University, Almaty, Kazakhstan*
**e-mail: morozzea@gmail.com*

Presented by Academician K.E. Degtyarev April 23, 2025

Received April 23, 2025; revised April 25, 2025; accepted April 28, 2025

Abstract—The results of the lithological and geochemical analysis of bottom sediments collected in the southwestern part of the Kara shelf in the area of development of gas-saturated deposits in a paleovalley at a depth of 112 m are presented. It has been established that the accumulation of the Holocene marine sediments occurred under conditions of fluid inflow as a result of degradation of permafrost and destruction of its gas hydrates, which are apparently suppliers of isotopically heavy waters to the studied strata.

Keywords: degassing, gas flares, seismoacoustics, gas hydrates, water isotopic composition, particle-size distribution analysis, permafrost

DOI: 10.1134/S1028334X25607345

The regime and rates of sedimentation in the southwestern part of the Kara shelf during the Late Pleistocene and Holocene have undergone frequent changes related to sea level fluctuations and variations in the degree of involvement of river and glacier runoff in sediment supply. Cryogenesis, which spread to the shelf areas during the Sartan period (18–23 kyr, MIS 2) was an additional factor that complicated the structure of the upper part of the sedimentary section. The issue of the position of the Kara Sea level during the last major regression remains contentious. There are opinions about the fall in the sea level to the current seabed levels of 30–50 m [1], 40–60 m [2], 110–130 m [3], etc. During the Holocene, the sea level gradually rose, and marine sediments began to accumulate in the flooded land areas. During the Holocene, sedimentation rates were laterally differentiated, and their quantitative estimates varied. The maximum rates in the central part of the southwestern sector of the Kara Sea did not exceed 0.5 mm/yr [4]. According to the data of isotopic dating, over the last 250 years, they have varied from 0.8–1.0 cm/yr in terrigenous-estuarine settings to 0.1–0.3 cm/yr in terrigenous-shallow marine environments in the southwestern part of the Kara shelf [5].

The study of the lithological composition and geochemistry of the Holocene sediments allows us to not only reconstruct their accumulation settings but also identify probable sources of sediment influx and the character of post-sedimentary changes in the sediment in situ, including those related to the degassing process, which is widely developed in the Arctic seas. Signs of fluid ascent in the upper part of the sedimentary cover and in the water column within the Barents-Kara region are well identified according to seismoacoustic data [6, 7]. At the same time, the character of the fluid ascent effect on the lithological and geochemical properties of the Holocene marine sediments has been studied locally in shelf settings. For instance, the studies of the sediment core in the region of southwestern Kara Sea adjacent to Yamal established that fluids contain freshwater, which is generated as a result of permafrost degradation [8].

The neoformation of authigenic carbonates, particularly ikaite, in bottom sediments is considered to be one of the indicators of fluid discharge. Ikaite is quite typical in the sediments of the cold-water seas [9], is formed under reducing conditions and indicates the presence of free gas in the sediments [6]. In particular, ikaites in the central part of the Kara shelf were detected at the same depths where seismoacoustic

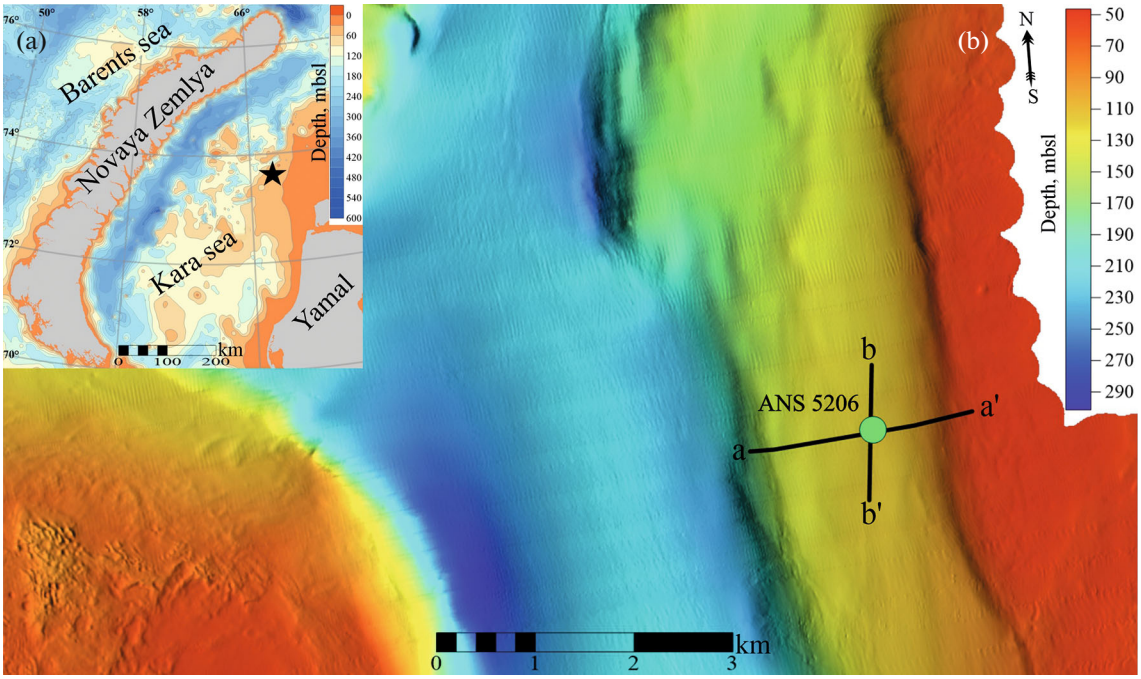

Fig. 1. (a) Location of the test site (marked with a star) and (b) digital terrain model of the seabed.

profiles often showed bright spots, interpreted as a gas front or the permafrost roof [6]. The ikaites found in the bottom sediments of the Arctic seas may indicate the ongoing processes of permafrost degradation [10].

The aim of this work was to reconstruct the conditions of bottom sediment formation within the area of development of gas-saturated deposits on the slope of a large paleovalley in the southwestern part of the Kara shelf and to identify the potential contribution of the permafrost degradation to fluid influx.

We used the bathymetric data acquired using a Reson Seabat 8111 multibeam echosounder system with a signal frequency of 100 kHz during cruise 52 of the R/V *Akademik Nikolaj Strakhov* in 2021. Acoustic profiling was performed using a Parasound P-35 profiler with signal frequencies of 4–8 kHz (the sedimentary cover) and 18–21 kHz (the water column). The process of detection and picking of acoustic anomalies related to the presence of gas in the upper part of the sedimentary cover was carried out in Kingdom Suite 2015 software. The material from the examined core ANS5206 was collected using a gravity core sampler (UGT-147), was initially described at the research vessel laboratory, and then was collected along the entire length of the core by subcoring, was stored, and transported to the laboratory in a refrigerator.

A comprehensive analysis was carried out at the Heat and Mass Transfer Laboratory of the Geological Institute of the Russian Academy of Sciences and at the Department of Geomorphology and Paleogeography of the Faculty of Geography at Moscow State University. This analysis included measuring of magnetic susceptibility with a SM-30 hand-held kappameter; measuring of thermal conductivity by means of the Tempos device; determination of moisture content using the gravimetric method by oven drying at 105°C to a constant weight; calculation of the content of $CaCO_3$ (by decomposition with an addition of a 10% HCl solution); calculation of the organic matter content (by decomposition with an addition of H_2O_2); particle-size distribution analysis using an Analysette 22 MicroTec Plus laser particle sizer; extraction of pore waters and their isotopic analysis. During the isotopic analysis, the samples were collected from the inner part of the subcored area. Centrifugation was performed on the day of sample collection for 15 min at a rate of 3000 rpm, the samples were not heated above standard conditions. The extracted water (1–2 mL) was collected with a sterile syringe and placed in a vial with a 300 μL micro-insert. The isotopic analysis was conducted on a Picarro L2140i infrared laser spectrometer. The standards used at the laboratory were USGS-46, USGS-47, USGS-48, as well as internal laboratory standards, including BRZ-21 ($\delta D = -133.21‰$; $\delta^{18}O = -18.27‰$), F-21 ($\delta D = -41.9‰$; $\delta^{18}O = -6.36‰$) and M-21 ($\delta D = 1.5‰$; $\delta^{18}O = 0.49‰$), calibrated relative to V-SMOW. The measurement accuracy was up to 0.05‰ for $\delta^{18}O$ and up to 0.2‰ for δD.

RESULTS

The sediment core ANS5206 (74.0577 N, 67.2726 E) with a thickness of 3.35 m was sampled at a depth of

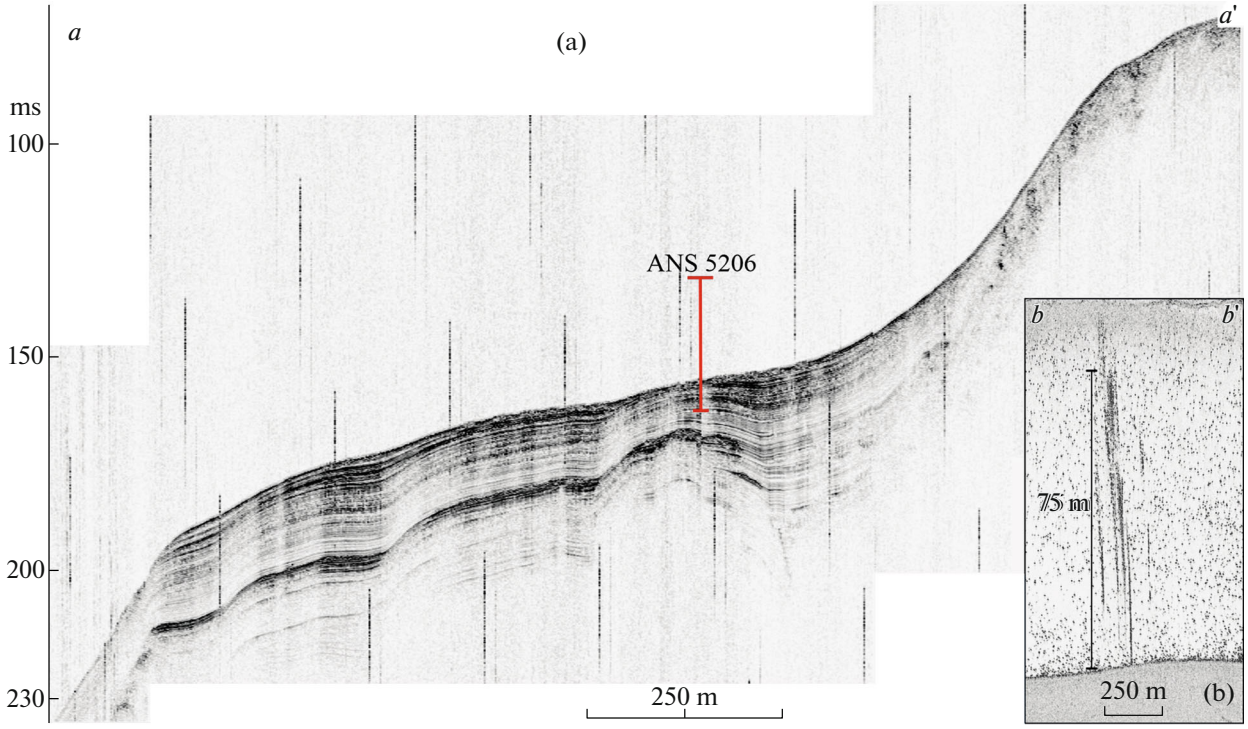

Fig. 2. (a) Seismoacoustic profile and location of core ANS5206; (b) flare-type acoustic anomalies within one strata. Profile positions are shown in Fig. 1.

112 m within a submeridionally elongated depression (a submerged paleovalley) cutting through the northern slope of the Rusanovskaya structural terrace west of the Yamal-Gydan shoal (Fig. 1a). The paleovalley has well-defined edges, is 5–6 km wide, and up to 250 m deep. A terrace-like surface manifests itself on its eastern slope at a depth of 110–115 m (Fig. 1b). The composing sediments are characterized by good acoustic stratification in the upper part (Fig. 2a). At a depth of ~10 m, the seismoacoustic data were used to reveal the "bright spot" anomaly (a gas front), below which acoustic blanking is recorded. The signs of degassing are also noted in the water column above the terrace-like surface. They manifest themselves as the "flare"-type acoustic anomalies (20–30 m high) and the areas of increased acoustic turbidity in the water (Fig. 2b). Based on a set of seismoacoustic features, we suggest that in the study area the fluid ascends into the upper part of the sedimentary cover and into the water column. The core ANS5206 was collected directly from the described terrace-like surface at the site where the water column showed the "flare"-type anomalies. They were first recorded in 2021 and in 2023 for the second time during cruise 56 of the R/V *Akademik Nikolaj Strakhov*.

The recovered bottom sediment strata consist of four layers by particle-size composition and texture. The upper three layers (layers 1, 2, and 3; Fig. 3) are represented by olive and greenish-gray pelitic silts with admixtures of fine-grained sand, having a homogeneous and lenticular-beding textures. The lower layer (layer 4) is grayish-olive pelitic clay with a lenticular-bedding texture. The particle-size composition of the sediments is dominated by silt (fraction >5–50 μm). Its content is 55–80%. The clay fraction (<5 μm) varies from 15 to 25%, the content of the sand fraction is within 3–4%, decreasing to less than 1% in layer 4, and reaching 22 and 7.9% only in two intervals of 30–32 and 170–172 cm, respectively. The particle-size spectra of the studied sediments are unimodal with the peaks in the medium silt range.

Layer 1 contains polychaete tubes 2 mm in diameter and up to 15 cm long. Throughout the core, there are scattered inclusions and thin interlayers of hydrotroilite, an authigenic iron sulfide, which fills pores in the silt-clay sediments. The presence of hydrotroilite reflects changes in redox conditions during uneven sedimentation and the activity of anaerobic sulfate-reducing microorganisms [11]. Layers 2, 3, and 4 were found to contain single bivalve shells and detritus (at depths of 62 and 177 cm). At a depth of 187–190 cm, an ikaite crystal ($CaCO_3 \cdot 6H_2O$) measuring 6 × 2 × 2 cm was discovered in the core. Bubble inclusions and mounds were noted in layer 4 at a depth greater than 280 cm, which probably indicates gas emission as a result of decompression.

The content of carbonates in core ANS5206 varies down the section from 4 to 15%, forming a smooth

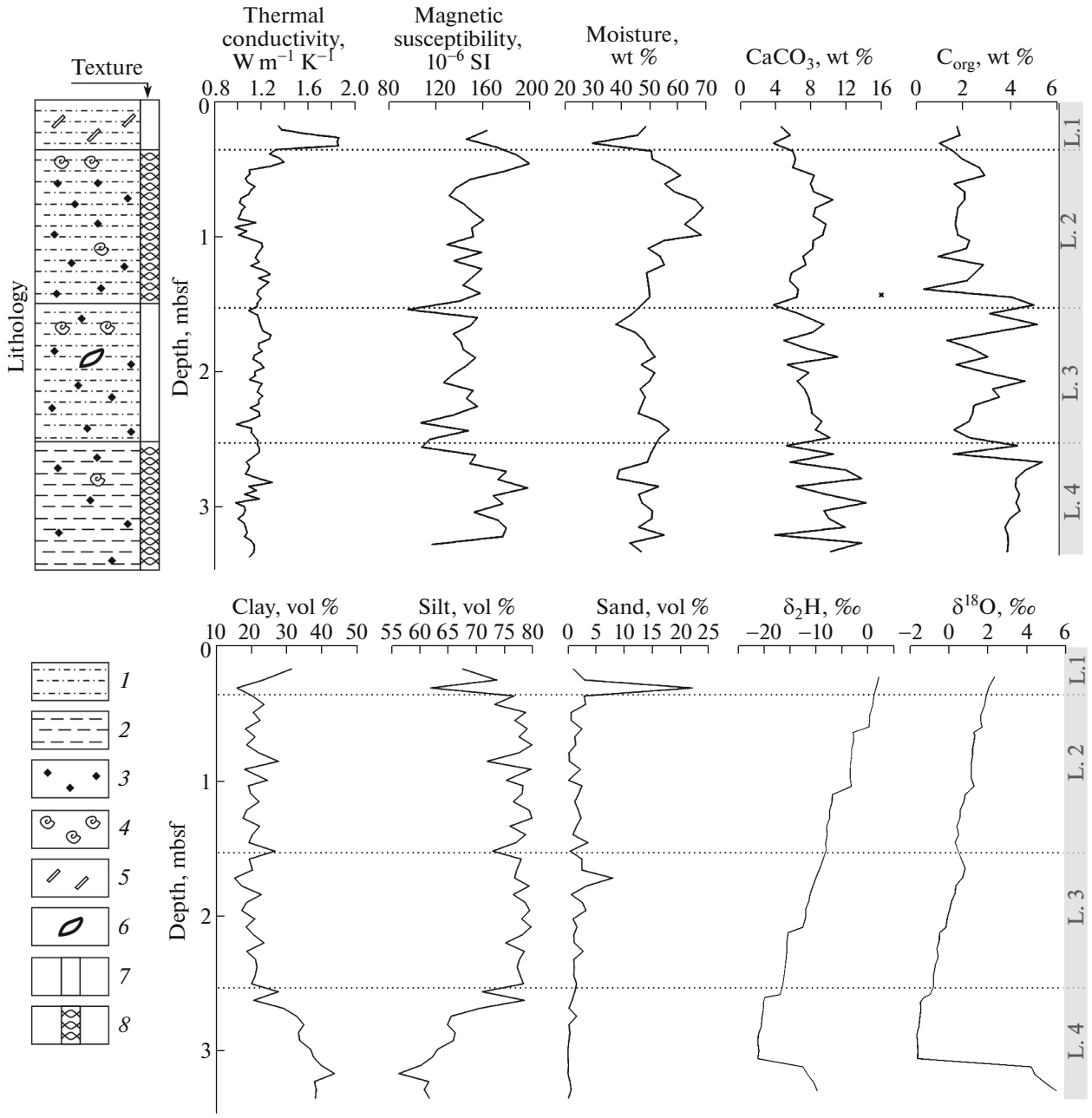

Fig. 3. Lithological composition, physicochemical properties, and isotopic composition of bottom sediments in core ANS5206. Legend: *1*, pelitic silt with an admixture of fine-grained sand; *2*, pelitic clay; *3*, hydrotroilite inclusions; *4*, shells and detritus; *5*, polychaete tubes; *6*, ikaite crystal; *7*, homogeneous sediment texture; *8*, lenticular-bedding sediment texture.

smeared peak in layer 2 in the upper part up to a depth of 1.5 m. Organic matter content increases with depth from 2 to 4–4.5%. Magnetic susceptibility is less than 16×10^{-5} SI units on average, with maxima up to 20×10^{-5} SI units in the upper 0.5 m and lower 1 m of the section. Thermal conductivity demonstrates a normal inverse dependence on moisture content. The isotopic composition is characterized by a gradual decrease in $\delta^{18}O$ and δD in layers 1, 2, and 3 and in the upper part of layer 4 ($\delta^{18}O$ varies from 2.3 to −1.6‰ and δD, from 2.1 to −21‰). A sudden increase in $\delta^{18}O$ to 5.51‰ and δD to −9.78‰ is recorded from a depth of 3.16 m to 3.34 m.

DISCUSSION

We distinguish two strata in the sedimentary cover studied in core ANS5206. The upper one, comprising layers 1, 2, and 3, is characterized by a relatively larger content of silt and fine-grained sand, a trend of

increasing contents of carbonate and organic matter down the section. In general, variability of properties increases down the section, which may indicate the more active hydrodynamic environment at the onset of the upper strata deposition (layer 3). The lower strata (layer 4) have higher clay content, density, almost complete absence of sand fractions, and increased content of organic matter. They were deposited under calmer hydrodynamic conditions. We can assume that layers 1, 2, and 3 were formed during the Holocene: the directed change in the lithological composition (particularly, in organic content) likely indicates gradual deepening of the basin during the transgression. A sand band recorded at the base of layer 1 probably implies the participation of bottom currents in sedimentation. Layer 4 was likely formed in a warmer environment with reduced hydrodynamics (perhaps during the Karginian period, 23–50 (55) ka BP, MIS 3). Due to high density and consequently low permeability, layer 4 is probably an impermeable layer, below which a gas front is detected at a depth of ~10 m on the seismoacoustic profile.

The occurrence of ikaite in the core, together with the recorded features of degassing on the seismoacoustic profiles, indicates both the possible presence of free gas in the sediments [6] and close to zero soil temperatures of soils. According to the available data [12], island permafrost rocks are widespread in the study area. They are recorded on the seismic profiles at depths of 50–60 m beyond the paleovalley edges and are likely absent at the bottom of the permafrost valley. The formation of ikaites in the bottom sediments is probably related to fluid inflow into the upper part of the section, including as a result of permafrost degradation in the adjacent shelf areas.

The isotopic composition of pore waters in bottom sediments differs significantly from that of waters in the Kara Sea open areas and from the fresh waters in the adjacent land [13]. The revealed isotopic enrichment of the water composition ($\delta^{18}O$ up to 5.51‰ and δD up to –9.78‰) in the upper and especially in the lower part of the core may be associated with the permafrost degradation and the destruction of its gas hydrates. Pore waters in hydrate-bearing layers [14] and bottom sediments in the fluid discharge areas are characterized by heavy isotopes [15]. The formation of ikaite in the sediments may also indicate the process of gas hydrate decomposition in the study area [16]. Besides, if we suppose that the terrace-like surface drainage occurred during the Sartan regression, then the isotopic enrichment of pore waters in layer 4 could also be related to the post-sedimentary processes under subaerial conditions (e.g., drying of the strata during freezing [17]). During the subsequent Holocene flooding, permafrost degraded, and marine water infiltrated the upper part of layer 4, leading to isotopic lightening. At the early stages of the transgression, the contribution of river runoff to sediment genesis was likely higher than in the later periods, which is indicated by the common trend in isotopic composition changes up the section. At the same time, the isotopic enrichment of the pore waters in layers 1 and 2 ($\delta^{18}O$ up to 2.3‰ and δD up to 2.2‰), which were accumulated in the marine environment during the Holocene, suggests that the values recorded in layer 4 cannot be explained only by subaerial cryogenesis. Both mechanisms could have contributed to the formation of the isotopic composition in the pore waters of the studied core.

CONCLUSIONS

The available data suggest that the Holocene marine sediments accumulated within the paleovalley in the southwestern part of the Kara shelf at depths of about 100 m under conditions of fluid influx as a result of the permafrost degradation and destruction of its gas hydrates. The continuous fluid influx to the seabed and the water column, recorded by the seismic data in 2021 and 2023, implies an ongoing degassing process that has an impact on the isotopic composition of the pore waters in the upper horizons of the sedimentary section.

ACKNOWLEDGMENTS

We are grateful to the crew of cruises 52 and 56 of the R/V *Akademik Nikolaj Strakhov* for their assistance in marine exploration.

FUNDING

This work was supported by the Russian Science Foundation, grant no. 22-77-10091 "Spatial Patterns of Degassing Manifestation on the Barents-Kara shelf and Its Influence on the Relief and Bottom Sediments."

CONFLICT OF INTEREST

The authors of this work declare that they have no conflicts of interest.

REFERENCES

1. I. D. Danilov and L. A. Zhigarev, in *Geographical Problem of the North Research* (Moscow State Univ., Moscow, 1977), pp. 115–135 [in Russian].
2. E. E. Musatov and G. N. Sokolov, Geomorfologiya, No. 2, 91–95 (1992).
3. Yu. I. Galushkin, Zhizn' Zemli, No. 4, 490–504 (2023).
4. V. S. Medvedev and E. M. Potekhina, in *Modern Sedimentation on the Shelf of World Ocean* (Moscow, 1990), pp. 110–120 [in Russian].
5. V. Yu. Rusakov, A. P. Borisov, and G. Yu. Solov'eva, Geochem. Int. **57** (11), 1185–1201 (2019).
6. E. A. Gusev, A. P. Matyushev, A. S. Rudoi, and A. N. Usov, in *Experience of System Oceanological Re-*

searches in Arctic, Ed. by A. P. Lisitsyn (Nauchn. mir, Moscow, 2001), pp. 553–558 [in Russian].

7. S. Yu. Sokolov, E. A. Moroz, G. D. Agranov, et al., Dokl. Earth Sci. **499** (2), 605–611 (2021).
8. P. Semenov, A. Portnov, A. Krylov, et al., Geochemistry **80** (3) (2020). https://doi.org/10.1016/j.chemer.2019.04.005
9. A. A. Krylov, E. A. Logvina, and E. A. Gusev, in *Proc. All-Russian Sci. Conf. "Fundamental Problems in the Study of Volcanogenic-Sedimentary, Terrigenous and Carbonate Complexes"* (GEOS, Moscow, 2023), pp. 85–87 [in Russian].
10. E. A. Logvina, A. A. Krylov, E. A. Gusev, et al., in *Proc. 14th Ural Lithological Meeting Heterogeneity in Sedimentary Systems* (Zavaritsky Inst. Geol. Geochem. Ural Branch RAS, Yekaterinburg, 2024), pp. 243–245 [in Russian].
11. V. I. Ferronsky, V. A. Polyakov, P. N. Kuprin, and L. S. Vlasov, Water Resour. **41** (4), 473 (2014).
12. A. V.Gavrilov, V. A. Pavlov, A. I. Fridenberg, et al., Neft. Khoz., No. 11, 28–32 (2019).
13. S. A. Kosova, Candidate's Dissertation in Geology and Mineralogy (Moscow, 2021).
14. M. V. Ivanov and A. P. Lein, *Biogeochemical Methane Cycle in the Ocean* (Nauka, Moscow, 2009) [in Russian].
15. V. N. Blinova, M. C. Comas, M. K. Ivanov, et al., Mar. Petrol. Geol. **28** (8), 1483–1504 (2011).
16. A. A. Krylov, E. A. Logvina, P. B. Semenov, et al., in *Proc. Ist Russian Gas Hydrates Conf. Gas Hydrates—Energy of the Future* (Listvyanka Settl., 2024), pp. 162–166 [in Russian].
17. V. N. Konishchev, V. V. Rogov, V. N. Golubev, and S. A. Sokratov, in *Proc. 4th Geocryologists Conf. in Russia* (Universitetskaya kniga, Moscow, 2011), pp. 71–74 [in Russian].

Translated by L. Mukhortova